Front. Phys., 2014, 9(4): 477–482
DOI 10.1007/s11467-014-0436-y

RESEARCH ARTICLE

Generation of adjustable pure spin currents in negative-U systems

Rui-Qiang Wang[1,†], **Li Sheng**[2], **Liang-Bin Hu**[1], **Mou Yang**[1], **Baigeng Wang**[2], **D. Y. Xing**[2]

[1] *Laboratory of Quantum Engineering and Quantum Materials, ICMP and SPTE, South China Normal University, Guangzhou 510006, China*

[2] *National Laboratory of Solid State Microstructures and Department of Physics, Nanjing University, Nanjing 210093, China*

Corresponding author. E-mail: † *rqwanggzu@163.com*

Received March 10, 2014; accepted April 24, 2014

Single-particle sequential tunneling is studied through a negative-U center hybridized with a superconducting, a ferromagnetic, and a normal metal electrodes. In stark contrast to the case of positive U, the single-particle tunneling in attractive charging energy is usually prohibited by ground states with electrons in pairs. We find a microscopic mechanism to induce single-particle sates from pair states. As a consequence, in the nonpolarized metal terminal a remarkable pure spin current with no charge currents survives over a wide range of gate- and bias- voltages, which is rather crucial for experimental observation and design of spintronic devices. In addition, a significant spin-filter effect is presented in certain bias regime.

Keywords spin current, negative U, proximity effect

PACS numbers 72.25.-b, 74.45.+c, 81.07.Nb

1 Introduction

Spintronic devices, utilizing spin degrees of freedom of electrons as carriers of information, are most promising to overcome the high power consumption and heating effect as compared to conventional charge-based electronic devices [1]. In the design of these devices, one of key technologies needed to be solved urgently is how to generate spin currents, especially pure spin currents without accompanying any charge currents. For this purpose, different methods have been put forward, such as the excitation of carriers with circularly polarized light [1], spin-Hall effect [2], and spin injection by electric or thermoelectric driving [3, 4].

In control of spins, the downscaling nanostructures, such as nanomagnets [5, 6] and shuttled dots [7, 8], possess great superiority attributed mainly to their unique intrinsic characteristics. The strong confinement in nanostructures leads to rich quantum effects, e.g., Kondo correlations [9–11] and spin phenomena [12–16]. Among those outstanding features, charging energy U plays a key role. The U is usually positive and repulses the spin-opposite electron pairs into the same orbit simultaneously. Conversely, the scenario of an Anderson model with negative U was reported recently in vibrated single molecules, defects, or impurity centers [17–21]. The negative U phenomenon was also realized in chemistry as inverse potential [22], or in some amorphous semiconductors [23] which was originally introduced to explain the magnetic properties of amorphous semiconductors.

The negative Coulomb correlations open up a unique transport way. The attractive interaction between electrons favors the occupation of nonmagnetic empty and doubly-occupied states because of their energies lower than the magnetic singly-occupied states. Thus, previous studies most focused on the transports dominated by pair tunnelings [17–19], which may develop the transports of electronic correlations in a degeneracy between two even-number charge states, and in turn lead to a charge-Kondo effect [21, 24, 25]. However, to our knowledge, there are hardly reports on the spintronics with respect to negative-U systems. It is naturally interesting to uncover the spin transports under negative U. To do this, it is crucial to induce a microscopic mechanism that can trigger the excitation of single-particle sates from pair states. In this paper, it is realized by coupling the negative-U center to an additional superconductor. Unexpectedly, a pure spin current without accompanying

Frontiers of Physics

any charge currents is obtained, which is adjustable over a wide range of gate- and bias- voltages.

2 Theory and formula

Let us first present above basic physics in a three-terminal Anderson impurity model, shown in Figs. 1(a) and (b). The single molecular orbit ε_0 with negative U is tunnel coupled to ferromagnetic (F), normal (N), and superconducting (S) electrodes. The electrochemical potential μ_α ($\alpha = \mathrm{F, N, S}$) is tuned to be $\mu_\mathrm{F} > \varepsilon_0 > \mu_\mathrm{N} > \varepsilon_0 + U$ with $\mu_\mathrm{S} = 0$ measured from the Fermi level E_F. If decoupled from the S lead, the molecule is eventually located in doubly-occupied level $\varepsilon_0 + U$ and so the single-electron transfer is prohibited. The introduction of superconductor can empty the electrons on the molecule, possibly followed by a crossed Andreev reflection (AR) via the lower level [Fig. 1(a)] or possibly by a sequential tunneling of single electrons via the upper level [Fig. 1(b)]. For N terminal, the former generates the backward electronic current while the latter gives forward one. Notice that the currents from the two processes have opposite spin orientation for each injected spin species, which provides a possibility to generate a pure spin current if two spin species is nonequivalent due to the F source.

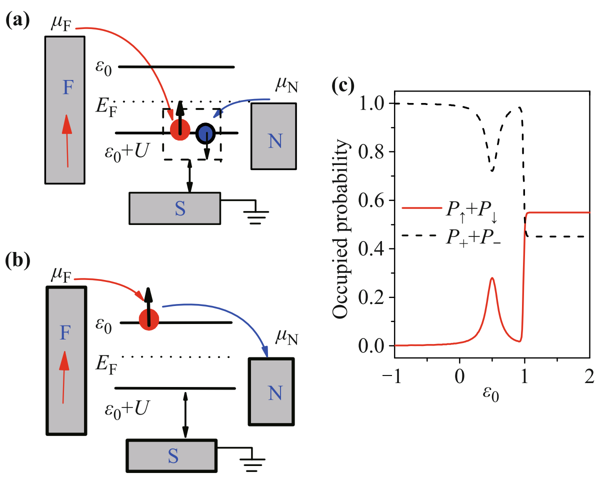

Fig. 1 Schematic diagrams for **(a)** crossed AR via level $\varepsilon_0 + U$ with two spin-opposite electrons from ferromagnetic (F) and normal (N) electrodes entering superconducting (S) electrode as a Cooper pair, and for **(b)** single-particle sequential tunneling via level ε_0. The level $\varepsilon_0 + U < \varepsilon_0$ is due to negative U. **(c)** Occupied probability $P_\uparrow + P_\downarrow$ for singly-occupied states and $P_+ + P_-$ for doubly-occupied states.

The electrodes ($\alpha = \mathrm{N, F}$) are described by Hamiltonian $H_\alpha = \sum_{k\sigma} \varepsilon_{\alpha k\sigma} c^\dagger_{\alpha k\sigma} c_{\alpha k\sigma}$, and the S electrode by s-wave BCS form $H_\mathrm{S} = \sum_{k\sigma} \varepsilon_{\mathrm{S}k\sigma} c^\dagger_{\mathrm{S}k\sigma} c_{\mathrm{S}k\sigma} - \sum_k (\Delta c^\dagger_{\mathrm{S}k_\uparrow} c^\dagger_{\mathrm{S},-k_\downarrow} + \Delta^* c_{\mathrm{S},-k_\downarrow} c_{\mathrm{S}k_\uparrow})$, where $c^\dagger_{\alpha k\sigma}$ is the creation operator for electrons with wave vector k and spin σ. The single-particle energy $\varepsilon_{\alpha k\sigma}$ is spin-dependent only for the F lead but spin-degenerate for the other leads ($\alpha = \mathrm{N, S}$). $\varDelta$ characterizes the superconducting pair potential. The Hamiltonian for the center is regarded as a well known Anderson–Holstein model with negative charging energy U, which can originate the strongly electron–phonon coupling molecule or the inverse potential impurities center [17, 20, 21], given by $H_\mathrm{M} = \sum_\sigma \varepsilon_0 d^\dagger_\sigma d_\sigma + U n_\uparrow n_\downarrow$, and the hopping term between the molecular level and leads is $H_\mathrm{T} = \sum_{\alpha,k\sigma} (t_{\alpha\sigma} c^\dagger_{\alpha k\sigma} d_\sigma + H.c.)$. Here, $n_\sigma = d^\dagger_\sigma d_\sigma$ is the number operator and $d^\dagger_\sigma$ creates a dot electron of energy ε_0, and $t_{\alpha\sigma}$ denotes the tunneling matrix element, relevant to tunnel-coupling strength $\varGamma_{\alpha\sigma} = 2\pi\rho_{\alpha\sigma}|t_{\alpha\sigma}|^2$ with $\rho_{\alpha\sigma}$ being the density of states of electrons in lead α.

We focus on the subgap transport by assuming infinite $\varDelta$. By integrating out the degrees of freedom of S lead as done in Refs. [14–16, 26, 27], one can obtain an effective molecular Hamiltonian as

$$H^\mathrm{eff}_\mathrm{M} = \sum_\sigma \varepsilon_0 d^\dagger_\sigma d_\sigma + U n_\uparrow n_\downarrow + \frac{\varGamma_\mathrm{S}}{2} d^\dagger_\uparrow d^\dagger_\downarrow + \frac{\varGamma_\mathrm{S}}{2} d_\downarrow d_\uparrow \quad (1)$$

Here, $\varGamma_\mathrm{S}$ plays a role of an effective local-pair potential on the molecule induced by proximity effect from superconductor. Diagonalizing $H^\mathrm{eff}_\mathrm{M}$ in Eq. (1) gives the many-body eigenstates: singly-occupied states $|\sigma\rangle$ with corresponding eigenvalues $\epsilon_{\uparrow(\downarrow)} = \varepsilon_0$, and doubly-occupied states $|\pm\rangle = \beta_\mp|0\rangle \mp \beta_\pm|\uparrow\downarrow\rangle$ with corresponding eigenvalues $\epsilon_\pm = (2\varepsilon_0 + U)/2 \pm \varepsilon_A$. $|\pm\rangle$ is a superposition state of $|0\rangle$ and $|\uparrow\downarrow\rangle$ with the weight factor $\beta_\pm = \frac{1}{\sqrt{2}}\sqrt{1 \pm (2\varepsilon_0 + U)/(2\varepsilon_A)}$ and $\varepsilon_A = \frac{1}{2}\sqrt{(2\varepsilon_0 + U)^2 + \varGamma^2_\mathrm{S}}$. Obviously, for $\varGamma_\mathrm{S} = 0$ the states $|-\rangle$ and $|+\rangle$ reduce to the empty $|0\rangle$ and doubly-occupied states $|\uparrow\downarrow\rangle$, respectively.

We focus on the regime of weak coupling to non-superconducting leads, where the sequential tunneling dominates the particle transports and the cotunneling is suppressed heavily. In the presentation of four basis states $|n\rangle \in |-\rangle, |\uparrow\rangle, |\downarrow\rangle, |+\rangle$, the occupied probability $P_n(t)$, standing for the probability of finding the molecule in state $|n\rangle$ at time t, is given by the dynamical Master equation [28]:

$$\frac{\partial P_n(t)}{\partial t} = \sum_{m\neq n,\alpha,\sigma} P_m(W^{\alpha\sigma+}_{n\leftarrow m} + W^{\alpha\sigma-}_{n\leftarrow m}) - P_n(W^{\alpha\sigma+}_{m\leftarrow n} + W^{\alpha\sigma-}_{m\leftarrow n}) \quad (2)$$

Here, the transition rates $W^{\alpha\sigma+}_{m\leftarrow n} = \varGamma_{\alpha\sigma} f_\alpha(\epsilon_m - \epsilon_n) \left|\langle m| c^\dagger_\sigma |n\rangle\right|^2$ and $W^{\alpha\sigma-}_{m\leftarrow n} = \varGamma_{\alpha\sigma}[1 - f_\alpha(\epsilon_n - \epsilon_m)] \left|\langle m| c_\sigma |n\rangle\right|^2$ relate to the electron tunneling into and out of the molecule, accompanied by the change of dot states from $|n\rangle$ to $|m\rangle$. $f_\alpha(\varepsilon) = 1/[1 + \mathrm{e}^{(\varepsilon-\mu_\alpha)/(k_\mathrm{B}T_\alpha)}]$ is the Fermi–Dirac distribution with $\mu_\alpha(T_\alpha)$ as the chemical potential (temperature) in lead α. For $\alpha = \mathrm{F}$, the spin splitting of ferromagnetism in density of states is reflected through spin polarization χ, defined as $\chi = (\rho_{\mathrm{F}\uparrow} - \rho_{\mathrm{F}\downarrow})/(\rho_{\mathrm{F}\uparrow} + \rho_{\mathrm{F}\downarrow})$, and thus one can label $\Gamma_{\mathrm{F}\uparrow(\downarrow)} = \Gamma_{\mathrm{F}}(1 \pm \chi)$.

We are interested in how the currents in N lead can be spin-polarized. Its steady-state spin-resolved currents are calculated by

$$I_{\mathrm{N}}^{\sigma} = \frac{-e}{h}\sum_{n,m}(W_{m\leftarrow n}^{\mathrm{N}\sigma+} - W_{m\leftarrow n}^{\mathrm{N}\sigma-})P_n \tag{3}$$

where P_n is obtained by setting $\partial P_n(t)/\partial t = 0$ in Eq. (2) under the normalization condition $\sum_n P_n = 1$.

3 Results and discussion

In this section, we will perform numerical calculations for the currents in N lead by assuming symmetric coupling $\Gamma_{\mathrm{N}\sigma} = \Gamma_{\mathrm{F}} = \Gamma_0$ with $\Gamma_0 < k_{\mathrm{B}}T_\alpha$. Set $U = -1$ and its absolute value as units of energy, $\Gamma_{\mathrm{S}} = 0.2$, $\chi = 0.6$, $k_{\mathrm{B}}T_\alpha = 0.01$, and $\mu_{\mathrm{F}} = 3$ throughout except for specific indication. The spin-dependent currents $I_{\mathrm{N}}^{\uparrow}$ and $I_{\mathrm{N}}^{\downarrow}$ are plotted in Fig. 2 as a function of molecular level ε_0, adjustable by gate voltage. We start with discussion of the case of the molecule disconnected from the S lead ($\Gamma_{\mathrm{S}} = 0$) in Fig. 2(a), for which a most prominent feature is appearance of a current step at ε_0 determined by $\varepsilon_0 + U = \mu_{\mathrm{N}}$ (i.e., $\varepsilon_0 = 2$ for chosen parameters), which is associated with the transition energy between states $|\uparrow\downarrow\rangle$ and $|\sigma\rangle$. Notice that another resonance at $\varepsilon_0 = \mu_{\mathrm{N}}$ drops, in contrast to the usual case of $U > 0$. The reason is that the single-particle transition between $|\sigma\rangle$ and $|0\rangle$ is blockaded by already saturated occupation in low-lying doubly-occupied states. As $\varepsilon_0 + U > \mu_{\mathrm{N}}$, all levels are within the bias window and the curves are equivalent to the results of $U = 0$, where the currents originate from the single-particle sequence tunneling with current polarization $\xi_1 = \frac{p}{2-p^2} \approx 0.36$ defined by $\xi = (I_{\mathrm{N}}^{\uparrow} - I_{\mathrm{N}}^{\downarrow})/(I_{\mathrm{N}}^{\uparrow} + I_{\mathrm{N}}^{\downarrow})$. When the superconducting lead is coupled to the molecule (e.g., $\Gamma_{\mathrm{S}} = 0.2$), a distinct feature is appearance of an additional negative-value peak around the particle-hole symmetric point $\varepsilon_0 = -U/2$. Away from this region, the currents almost recover the zero value. The current peak completely attributes to the AR since in this region the single-particle tunneling from F to N lead via the molecule is blockaded. The AR reaches the maximum at the symmetric point $\varepsilon_0 = -U/2$. Furthermore, the AR currents $I_{\mathrm{N}}^{\uparrow} \neq I_{\mathrm{N}}^{\downarrow}$ is spin-polarized with polarization maximum only slightly lower than ξ_1 for the sequential tunneling, which implies the crossed AR is in this region dominant over the local AR with respect to single N lead.

As μ_{N} is reduced, both spin-dependent AR current peaks are heavily suppressed but their positions pin at $\varepsilon_0 = -U/2$, accompanied with the current step moving to the left. Interestingly, the currents of two spin species shrink in different rate. As illustrated in Fig. 2(b) for $\mu_{\mathrm{N}} = 0.5$, $I_{\mathrm{N}}^{\uparrow}$ almost vanishes while $I_{\mathrm{N}}^{\downarrow}$ keeps finite, which exhibits a pronounced spin-filter effect. With μ_{N} decreasing further, $I_{\mathrm{N}}^{\uparrow}$ reverses quickly its sign to become a positive peak but $I_{\mathrm{N}}^{\downarrow}$ remains still a negative peak. Unexpectedly, in Fig. 2(c) for $\mu_{\mathrm{N}} = 0$ (not only limited to this point, see Fig. 3), an interesting finding is that the relation of $I_{\mathrm{N}}^{\uparrow} = -I_{\mathrm{N}}^{\downarrow}$ holds exactly and so there presents a large spin current $I_{\mathrm{N}}^{s} = 2I_{\mathrm{N}}^{\uparrow}$, defined as $I_{\mathrm{N}}^{s} = I_{\mathrm{N}}^{\uparrow} - I_{\mathrm{N}}^{\downarrow}$, together with a vanished charge current $I_{\mathrm{N}}^{c} = I_{\mathrm{N}}^{\uparrow} + I_{\mathrm{N}}^{\downarrow} = 0$. It is reminiscent of the case of $U \geqslant 0$ with the same setup [16, 29], in which a pure spin current can be obtained only by tuning ε_0 exactly at certain specific point. However, here the pure spin current appears in a broad parameter range of ε_0, which is rather crucial for experimental observation and design of spintronic devices. At low temperatures under consideration and in the vicinity of particle-hole symmetric point, $|U + 2\varepsilon_0| < \sqrt{U^2 - \Gamma_{\mathrm{S}}^2}$, the Fermi distribution functions reduce to be $f_{\mathrm{F}}(\varepsilon) \approx 1$ and $f_{\mathrm{N}}(\epsilon_\pm - \varepsilon_\sigma) \approx 1$. With these, we derive simple analytic expressions of the spin-resolved currents as $I_{\mathrm{N}}^{\uparrow} = \frac{\Gamma_0\Gamma_{\mathrm{S}}^2\chi}{3\Gamma_{\mathrm{S}}^2+(3-\chi^2)(U+2\varepsilon_0)^2}$ and $I_{\mathrm{N}}^{\downarrow} = -I_{\mathrm{N}}^{\uparrow}$. At symmetric point $\varepsilon_0 = -U/2$, they further reduce to $I_{\mathrm{N}}^{\uparrow} = -I_{\mathrm{N}}^{\downarrow} = \Gamma_0\chi/3$ and so the pure spin current is $I_{\mathrm{N}}^{s} = 2\Gamma_0\chi/3$, regardless of the Γ_{S}. In contrast, our numerical calculations for positive U shown in

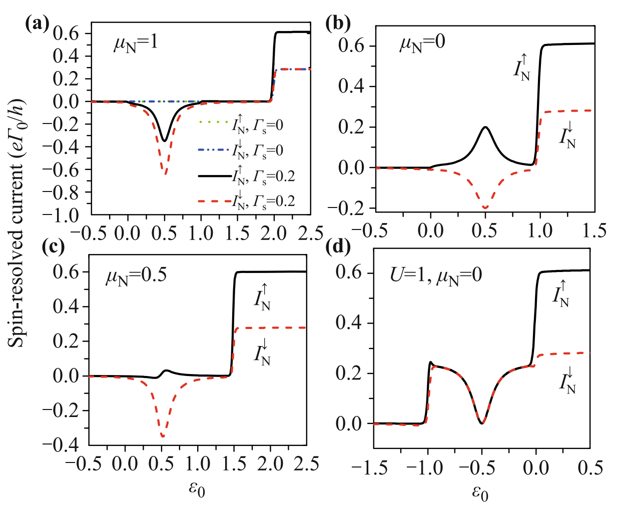

Fig. 2 Spin-resolved current I_{N}^{σ} as a function of molecular level ε_0 for electrochemical potential **(a)** $\mu_{\mathrm{N}} = 1$, **(b)** $\mu_{\mathrm{N}} = 0.5$, and **(c)** $\mu_{\mathrm{N}} = 0$. **(d)** The case of positive $U = 1$ is plotted for comparison with (c).

Fig. 2(d) indicate that the currents of two species are spin degenerate in the vicinity of degeneracy point due to nonequilibrium spin accumulations [30]. At low temperatures they are derived analytically to be $I_{\rm N}^{\uparrow} = I_{\rm N}^{\downarrow} = \frac{\Gamma_0(1-\chi^2)(U+2\varepsilon_0)^2}{3\Gamma_{\rm S}^2+(3-\chi^2)(U+2\varepsilon_0)^2}$ where the spin current vanishes for $U > 0$.

We want to address that $I_{\rm N}^{\uparrow} = -I_{\rm N}^{\downarrow}$ near the symmetric point $\varepsilon_0 = -U/2$ in Fig. 2(c) is a consequence of joint effect of the crossed AR and AR-governed single-particle tunneling. The unique process to open single-particle channels can be seen from Fig. 1(c), where nonzero probability $P_{\uparrow} + P_{\downarrow}$ of singly-occupied states $|\sigma\rangle$ arises only near the AR regime, induced by reduction of the probability $P_+ + P_-$ of doubly-occupied states $|\pm\rangle$. This is in sharp contrast to the case of $U > 0$, where $|\sigma\rangle$ is favorable first and then followed by $|\pm\rangle$. Thus, we can understand the underlying physics simply as follows. When a spin-σ electron is injected from F lead each time the molecular level is empty, the probability to jump onto the lower level is the same as that onto the upper level, the former followed by the crossed AR current $I_{{\rm N},\bar{\sigma}}^{\rm AR}$ with $\bar{\sigma}$ opposite to σ [Fig. 1(a)] and the latter followed by the sequential tunneling current $I_{{\rm N},\sigma}^{\rm seq}$ [Fig. 1(b)]. As a consequence the relation of $I_{{\rm N},\sigma}^{\rm seq} = -I_{{\rm N},\bar{\sigma}}^{\rm AR}$ holds in N lead. Each spin component contains the two processes simultaneously, i.e., $I_{\rm N}^{\sigma} = I_{{\rm N},\sigma}^{\rm seq} + I_{{\rm N},\sigma}^{\rm AR} = I_{{\rm N},\sigma}^{\rm seq} - I_{{\rm N},\bar{\sigma}}^{\rm seq}$, resulting in $I_{\rm N}^{\uparrow} = -I_{\rm N}^{\downarrow}$.

Next, we analyze the sensitivity of pure spin current to other systemic parameters. In Figs. 3(a) and (b), we display the numerical results of spin-resolved currents $I_{\rm N}^{\sigma}$ for different χ and $\Gamma_{\rm S}$, respectively. It is found that when either χ or $\Gamma_{\rm S}$ is absent, the currents are suppressed to be zero. The absolute hight of spin-dependent current peaks is determined by χ, regardless of $\Gamma_{\rm S}$, while the width is mainly by $\Gamma_{\rm S}$. Even for quite weak but not vanished $\Gamma_{\rm S}$ (e.g., $\Gamma_{\rm S} = 10^{-2}$), $I_{\rm N}^{\sigma}$ can still reach the maximum $\Gamma_0\chi/3$. However, in order to observe the pure spin current in a broader parameter range, enhancing $\Gamma_{\rm S}$ is necessary. Meantime, it is noticed that for larger $\Gamma_{\rm S}$ (e.g., $\Gamma_{\rm S} = 0.4$), $I_{\rm N}^{\uparrow}$ and $I_{\rm N}^{\downarrow}$ far away from the symmetric point $\varepsilon_0 = -U/2$ are no longer exactly equal because the local AR relevant to single N lead contributes to transports, generating non-zero charge currents. The variation of $I_{\rm N}^{\sigma}$ with $\mu_{\rm N}$ is illustrated in Figs. 3(c) for $\Gamma_{\rm S} = 10^{-3}$ and (d) for $\Gamma_{\rm S} = 0.2$, where we set $\varepsilon_0 = -U/2$. Again, $I_{\rm N}^{\uparrow}$ and $I_{\rm N}^{\downarrow}$ are strictly symmetric about the horizon axis roughly in the region of $\mu_{\rm N} \in [\frac{U}{2}, -\frac{U}{2}]$ in Fig. 3(c), with constant value $|I_{\rm N}^{\uparrow(\downarrow)}| = \Gamma_0\chi/3$. Increasing $\Gamma_{\rm S}$ as in Fig. 3(d) brings $I_{\rm N}^{\sigma}$ with two new plateaus, respectively, in the range of $|\mu_{\rm N} \pm \varepsilon_0| \leqslant \varepsilon_A$ whose width is just the magnitude of $\Gamma_{\rm S}$. These new plateaus originate from the level splitting of $\varepsilon_+ - \varepsilon_- = 2\varepsilon_A = \Gamma_{\rm S}$ for $\varepsilon_0 = -U/2$. This is in contrast with $U > 0$, where the current $I_{\rm N}^{\uparrow(\downarrow)} = 0$ for $\mu_{\rm N} \in [-\frac{U}{2}, \frac{U}{2}]$ due to the AR channel being Coulomb blocked.

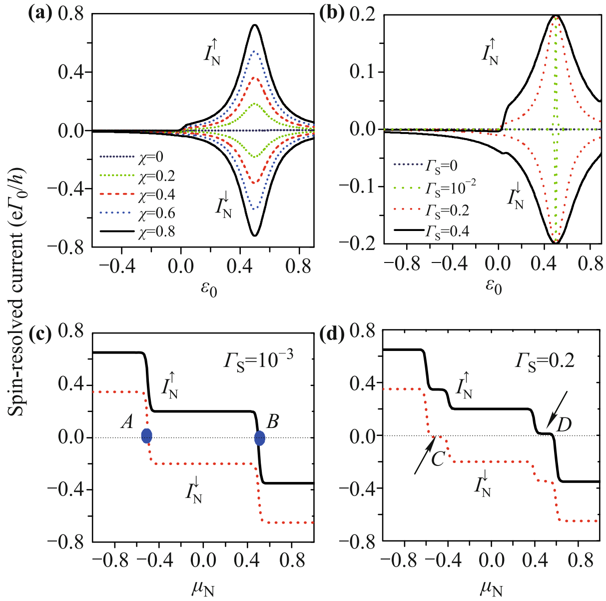

Fig. 3 $I_{\rm N}^{\sigma}$ as a function of ε_0 for **(a)** different spin polarization χ and **(b)** different $\Gamma_{\rm S}$; the curves of $I_{\rm N}^{\uparrow}$ ($I_{\rm N}^{\downarrow}$) being above (below) horizon axis. Variation of $I_{\rm N}^{\sigma}$ with $\mu_{\rm N}$ in the symmetric point $\varepsilon_0 = -U/2$ for **(c)** $\Gamma_{\rm S} = 10^{-3}$ and **(d)** $\Gamma_{\rm S} = 0.2$. Positions indicated by A, B, C, and D exhibit a remarkable spin-filter effect.

Finally, it is also interesting to find that at points indicated by A and B in Fig. 3(c), one of spin-dependent currents is vanished but the other spin component has finite value, exhibiting a significant spin-filter effect. This spin-filter effect is also observable in Fig. 2(b). Increasing $\Gamma_{\rm S}$ broadens the points A and B into two zero-current plateaus, as shown by C and D in Fig. 3(d), making the spin-filter effect exist in a wider range of $\mu_{\rm N}$. Notice that the pure spin current between C and D is related to the AR-induced single-particle tunneling while the currents out of this regime is due to direct single-particle tunneling. It is just the transition of two tunneling mechanisms that leads to appearance of the spin-filter effect.

4 Conclusions

In conclusion, we theoretically study the spin-dependent transports through a molecule with negative U in a three-terminal setup. Unlike the case of repulse charging energy, the attractive one prohibits the single-particle tunneling due to the ground states of molecules being occupied with even-number electrons. Particular attention is paid to the regime where the single-occupied level is within the F-N bias window while the doubly-occupied level is out of it. In this bias regime, we find a microscopic mechanism to excite single-particle sates by crossed AR process. Interestingly, the opening of the single-particle tunneling is determined completely by the AR process. As a consequence of their joint effect, near particle-hole degeneracy point, the generating currents in N lead have opposite moving directions but with the same magnitude for different spins, exhibiting a remarkable pure spin current. The most striking superiority is its existence in a wide range of bias- and gate- voltages, which is rather crucial for experimental observation and design of spintronic devices. In addition, we also find a remarkable spin-filter effect when tuning the gate voltage or bias to be certain value. The proposed generator of pure spin currents can be realized experimentally by means of existing nanofabrication techniques [31].

Acknowledgements This work was supported by the Program for New Century Excellent Talents in University (NCET) of China (Grant No. NCET-10-0090), the National Natural Science Foundation of China (Grant Nos. 11174088 and 11274124), the State Key Program for Basic Researches of China (Grant Nos. 2006CB921803 and 2010CB923400), the Program for Changjiang Scholars and Innovative Research Team in University (PCSIRT) (Grant No. IRT1243), and the Natural Science Foundation of Guangdong Province of China (Grant No. S2012010010681).

References

1. I. Žutić, J. Fabian, and S. D. Sarma, Spintronics: Fundamentals and applications, *Rev. Mod. Phys.*, 2004, 76(2): 323
2. Y. K. Kato, R. C. Myers, A. C. Gossard, and D. D. Awschalom, Observation of the spin Hall effect in semiconductors, *Science*, 2004, 306(5703): 5703
3. F. J. Jedema, A. T. Filip, and B. J. van Wees, Electrical spin injection and accumulation at room temperature in an all-metal mesoscopic spin valve, *Nature*, 2001, 410(6826): 345
4. K. Uchida, S. Takahashi, K. Harii, J. Ieda, W. Koshibae, K. Ando, S. Maekawa, and E. Saitoh, Observation of the spin Seebeck effect, *Nature*, 2008, 455(7214): 778
5. A. R. Rocha, V. M. Garciá-Suárez, S. W. Bailey, C. J. Lambert, J. Ferrer, and S. Sanvito, Towards molecular spintronics, *Nat. Mater.*, 2005, 4(4): 335
6. L. Bogani and W. Wernsdorfer, Molecular spintronics using single-molecule magnets, *Nat. Mater.*, 2008, 7(3): 179
7. D. Fedorets, L. Y. Gorelik, R. I. Shekhter, and M. Jonson, Spintronics of a nanoelectromechanical shuttle, *Phys. Rev. Lett.*, 2005, 95(5): 057203
8. R. Q. Wang, B. G. Wang, and D. Y. Xing, Spin valve effect in a magnetic nanoelectromechanical shuttle, *Phys. Rev. Lett.*, 2008, 100(11): 117206
9. B. K. Kim, Y. H. Ahn, J. J. Kim, M. S. Choi, M. H. Bae, K. Kang, J. S. Lim, R. Lopez, and N. Kim, Transport measurement of Andreev bound states in a Kondo-correlated quantum dot, *Phys. Rev. Lett.*, 2013, 110(7): 076803
10. A. Martín-Rodero and A. L. Yeyati, Josephson and Andreev transport through quantum dots, *Adv. Phys.*, 2011, 60(6): 899
11. A. Oguri, Y. Tanaka, and J. Bauer, Interplay between Kondo and Andreev–Josephson effects in a quantum dot coupled to one normal and two superconducting leads, *Phys. Rev. B*, 2013, 87(7): 075432
12. W. Chang, V. E. Manucharyan, T. S. Jespersen, J. Nygard, and C. M. Marcus, Tunneling spectroscopy of quasiparticle bound states in a spinful josephson junction, *Phys. Rev. Lett.*, 2013, 110(21): 217005
13. C. Richard, M. Houzet, and J. S. Meyer, Andreev current induced by ferromagnetic resonance, *Phys. Rev. Lett.*, 2012, 109(5): 057002
14. B. Sothmann, D. Futterer, M. Governale, and J. König, Probing the exchange field of a quantum-dot spin valve by a superconducting lead, *Phys. Rev. B*, 2010, 82(9): 094514
15. D. Futterer, M. Governale, M. G. Pala, and J. König, Nonlocal Andreev transport through an interacting quantum dot, *Phys. Rev. B*, 2009, 79(5): 054505
16. D. Futterer, M. Governale, and J. König, Generation of pure spin currents by superconducting proximity effect in quantum dots, *Europhys. Lett.*, 2010, 91(4): 47004
17. J. Koch, M. E. Raikh, and F. von Oppen, Pair tunneling through single molecules, *Phys. Rev. Lett.*, 2006, 96(5): 056803
18. J. Koch and F. von Oppen, Franck-Condon blockade and giant Fano factors in transport through single molecules, *Phys. Rev. Lett.*, 2005, 94(20): 206804
19. K. I. Wysokiński, Thermal transport of molecular junctions in the pair tunneling regime, *Phys. Rev. B*, 2010, 82(11): 115423
20. N. T. Son, X. T. Trinh, L. S. Lovlie, B. G. Svensson, K. Kawahara, J. Suda, T. Kimoto, T. Umeda, J. Isoya, T. Makino, T. Ohshima, and E. Janzen, Negative-U system of carbon vacancy in 4H-SiC, *Phys. Rev. Lett.*, 2012, 109(18): 187603
21. T. A. Costi and V. Zlatic, Charge Kondo anomalies in PbTe doped with Tl impurities, *Phys. Rev. Lett.*, 2012, 108(3): 036402
22. C. Kraiya and D. H. Evans, Investigation of potential inversion in the reduction of 9,10-dinitroanthracene and 3,6-dinitrodurene, *J. Electroanal. Chem.*, 2004, 565(1): 29
23. P. W. Anderson, Model for the electronic structure of amorphous semiconductors, *Phys. Rev. Lett.*, 1975, 34(15): 953
24. J. Koch, E. Sela, Y. Oreg, and F. von Oppen, Nonequilibrium charge-Kondo transport through negative-U molecules, *Phys. Rev. B*, 2007, 75(19): 195402
25. P. S. Cornaglia, H. Ness, and D. R. Grempel, Many-body effects on the transport properties of single-molecule devices, *Phys. Rev. Lett.*, 2004, 93(14): 147201

26. P. Recher, Y. V. Nazarov, and L. P. Kouwenhoven, Josephson light-emitting diode, *Phys. Rev. Lett.*, 2010, 104(15): 156802

27. T. Meng, S. Florens, and P. Simon, Self-consistent description of Andreev bound states in Josephson quantum dot devices, *Phys. Rev. B*, 2009, 79(22): 224521

28. C. Timm, Tunneling through molecules and quantum dots: Master-equation approaches, *Phys. Rev. B*, 2008, 77(19): 195416

29. Z. Chen, B. G. Wang, D. Y. Xing, and J. Wang, A spin injector, *Appl. Phys. Lett.*, 2004, 85(13): 2553

30. F. M. Souza, J. C. Egues, and A. P. Jauho, Quantum dot as a spin-current diode: A master-equation approach, *Phys. Rev. B*, 2007, 75(16): 165303

31. S. De Franceschi, L. Kouwenhoven, C. Schönenberger, and W. Wernsdorfer, Hybrid superconductor–quantum dot devices, *Nat. Nanotechnol.*, 2010, 5(10): 703